Article

J. Mex. Chem. Soc. **2009**, *53(2),* 59-70

ISSN 1870-249X

Study of Sorption Equilibrium of Biopolymers Alginic Acid and Xanthan with C.I. Disperse Yellow 54

Juan Antonio Lozano-Álvarez,[1] Juan Jáuregui-Rincón,[1*] Guillermo Mendoza-Díaz,[2] Refugio Rodríguez-Vázquez,[3] and Claudio Frausto-Reyes[4]

[1] Departamento de Ingeniería Bioquímica, Universidad Autónoma de Aguascalientes, Av. Universidad 940 Ciudad Universitaria, Aguascalientes, México. jjaureg@correo.uaa.mx
[2] Facultad de Química, Universidad de Guanajuato, Noria Alta S/N, Guanajuato, México.
[3] Centro de Investigación y de Estudios Avanzados del Instituto Politécnico Nacional, México, D.F., México.
[4] Centro de Investigaciones en Optica, Unidad Aguascalientes. Aguascalientes, México.

Received January 12, 2009; accepted June 29, 2009

Abstract. Disperse yellow 54 (DY54) was adsorbed onto two biopolymers, alginic acid and xanthan. The adsorption isotherms for the biopolymer-DY54 system showed that the adsorption mechanism can best be described by Zimm-Bragg theory. UV-Visible, FT-IR and MicroRaman studies suggest that DY54 is bounded to both biopolymers alginic acid and xanthan through hydrogen bonding. Keto group of dye and hydroxyl groups of sugar residues from two polysaccharides were the principal functional groups involved in sorption mechanism.
Keywords: Sorption, Biopolymers, Disperse dye, Zimm-Bragg Theory, Hydrogen Bonding.

Resumen. El colorante Amarillo disperso 54 (DY54) fue adsorbido en dos biopolímeros, el ácido algínico y la xantana. Las isotermas de adsorción obtenidas para el sistema biopolímero-DY54 muestran que el mecanismo de adsorción puede ser descrito de la mejor manera por la teoría de Zimm-Bragg. Estudios UV-Visible, IR-TF y MicroRaman sugieren que el DY54 se une a ambos biopolímeros, el ácido algínico y la xantana por medio de puentes de hidrógeno. El grupo cetónico del colorante y los grupos oxhidrilo de los residuos de azúcar de los dos polisacáridos fueron los principales grupos funcionales involucrados en el mecanismo de adsorción.
Palabras clave: Adsorción, biopolímeros, colorante disperso, teoría de Zimm-Bragg, puentes de hidrógeno.

Introduction

The textile industry throws wastewaters to municipal sewage system that, in spite of having processes of conventional aerobic treatment, still contain considerable amount of dyes [1]. Among these effluents disperse dyes predominate due to their little solubility in aqueous medium therefore present a greater difficulty in both their removal and degradation from the industrial effluents even if this last one is carried out by anaerobic way [2,3]. Although the research in the field of dissolution of disperse dyes in gases under supercritical conditions in an attempt to dyeing synthetic fibers is growing [4-10], still the application of disperse dyes is through wet route using dispersant agents that facilitates the adsorption of dye in substrate [11]. Unfortunately the totality of dye is not transferred to the fiber and significant amounts of these untreated dyes are released to rivers, lakes and water receptors, without any modification in their structure. Disperse yellow 54 (DY54) whose structure is showed in Figure 1 is used in dyeing different synthetic fibers such as, polyester, polyamide, acrylic acetate and plastics [11,12].

Although some disperse dyes have shown be removed by different materials [13-16], few reports have been written concerning about the removal of these compounds using biopolymers. Alginic acid (ALG) is a polysaccharide produced by microorganisms (algae and bacteria) that is used principally in food industry as stabilizer, thickener and gelling agent. It is a linear polymer of β(1→4)-D-mannuronate (M) and α(1→4)-L-guluronate (G) [17] (Figure 2). A gel is formed when a divalent ion salt (principally Ca^{2+}) is added to a solution of alginic acid. Gel formation mechanism is described by the "egg box model" [18].

Xanthan (XANT) is an extracellular polysaccharide secreted by *Xanthomonas campestris* [19,20]. This anionic polyelectrolyte consists of a main cellulosic chain with trisaccharide side chains, each of which contains one glucuronyl and two mannosyl residues attached at the C-3 position on an alternate glucosyl residue (Figure 3). Each of the internal and terminal mannosyl residues of the side chain has an O-acetyl group at the C-6 position and a piruvate ketal at the C-4 and C-6 positions, respectively.

This biopolymer provides a degree of viscosity to the solution which is added and this property is maintained in a wide

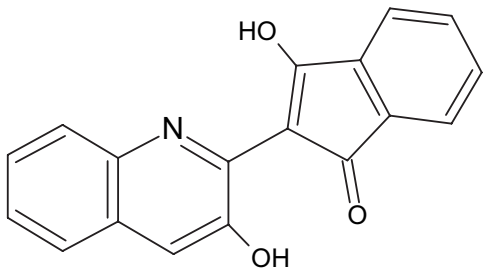

Fig. 1. Structure of disperse yellow 54 (DY54).

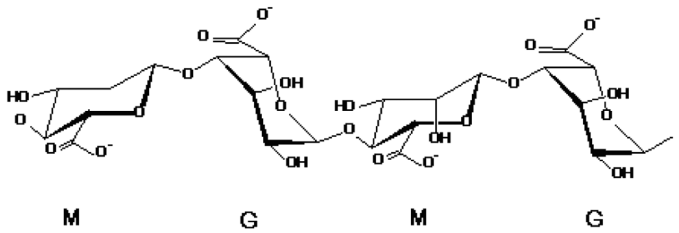

Fig. 2. Structure of Alginic acid.

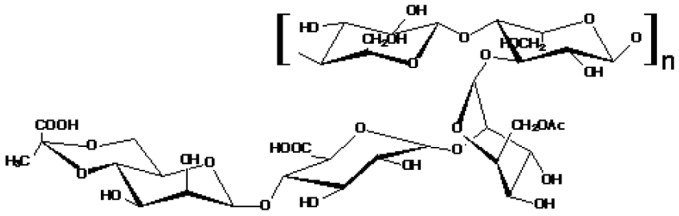

Fig. 3. Structure of xanthan.

pH range, stability of solutions of this polymer is enhanced with addition of some salts principally potassium chloride [19]. Because of its capacity to keep viscosity at adequate levels it is used in food industry and oil drilling industry.

In this work, sorption isotherms of DY54 with both biopolymers alginic acid and xanthan are reported. Spectroscopic studies (UV-Visible, FT-IR, and MicroRaman) help us to elucidate the functional groups involved in the sorption process. Within these results, we propose a mechanism for the interaction between the dye and each biopolymer.

Results and Discussion

The use of pure DY54 with biopolymers ALG and XANT allowed to obtain results where interferences generated from dyeing assistances (e.g. dispersant agent, salts, etc.) were eliminated and will allow us to understand the main interactions between the dye and these polysaccharides. For that purpose high performance liquid chromatography was used to check the purity of DY54 samples. Figure 4 shows the chromatogram of DY54 purified by column chromatography.

UV-Visible studies

The influence of pH on the absorption electronic spectrum of DY54 was determined (Figure 5). Two principal changes in signal peak were observed after pH modification: when pH moved from pH 10.99 to pH 11.25 maximum peak located at 376 was shifted to 373 nm. In the same way absorption signal at 223 was moved to 220 nm when pH changed from 11.25 to 11.78.

It is known that several compounds such as acid-base indicators [21,22], anthocianins [23] and eosin [24] suffer

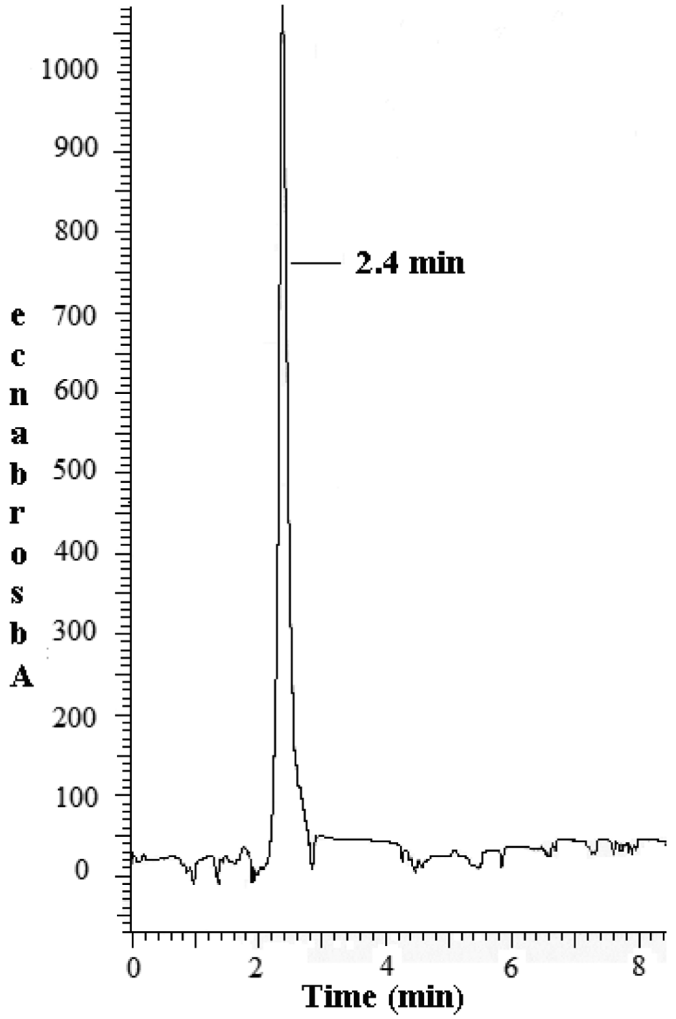

Fig. 4. HPLC chromatogram of DY54, for run conditions see experimental section.

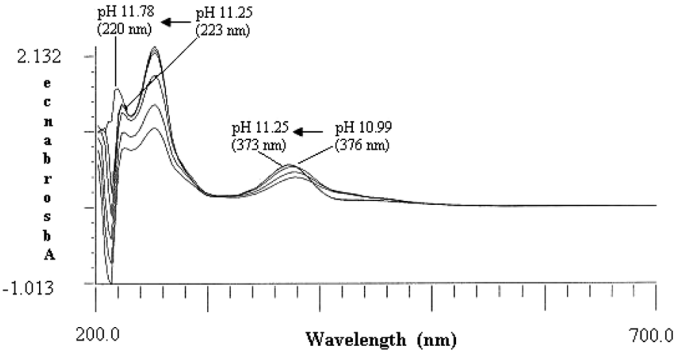

Fig. 5. UV-Visible absorption spectrum of DY54 in water at different pH values.

modifications in their electronic distribution due to protonation or deprotonation processes when pH is changed and in some cases this electronic rearrangement causes a color change. DY54 have two hydroxyl groups (Figure 1) that can be deprotonated when pH is moved from 10.99 (bright yellow) to 11.78

(reddish yellow), there is possible that pKa´s of hydroxyl groups of DY54 are localized in this pH range.

To obtain the possible effects of addition of biopolymers to DY54 absorption spectrum different aliquots of them were added to DY54 solution (Figures 6 and 7). When increasing concentration of alginic acid only dilution effect was observed. Not changes in signal peaks localization of DY54 spectrum were observed (Figure 6).

Pal and Mandal [25] reported that increasing amounts of potassium alginate added to 1,9-dimethylmethyleneblue and pinacyanol solutions produced an induction of metachromasia (changes in ubication of maximal peaks) in the spectra of these dyes. This indicates that aggregates formed by the dyes in aqueous solution were disrupted by the interaction between biopolymer and them. The results suggest that interaction between dye and biopolymer is so weak that no structural change in DY54 molecule is observed.

In the case of XANT-DY54 system occurred a similar finding than the one found in ALG-DY54 system (Figure 7). The only difference was an increase in signal intensity for signal at 220 nm when xanthan concentration was increased but this modification in spectrum was due to xanthan itself (see figure 8) rather than a possible interaction between DY54 and this biopolymer.

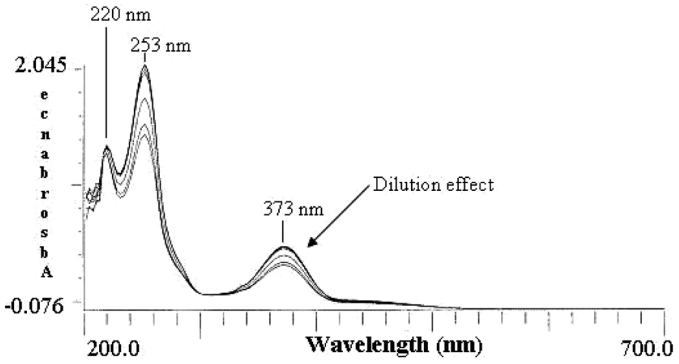

Fig. 6. UV-Visible absorption spectra of Dy54 when alginate solution (1% w/v) was added.

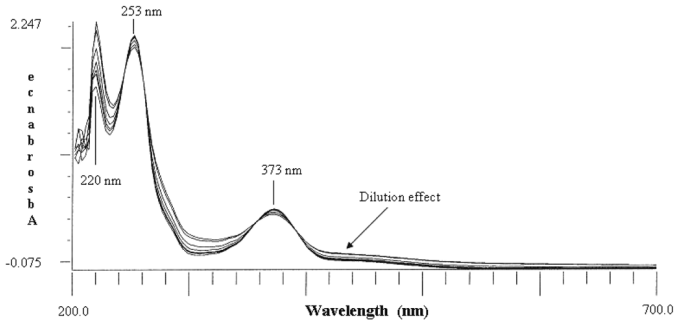

Fig. 7. UV-Visible absorption spectra of Dy54 when xanthan solution (1% w/v) was added.

Sorption studies

The influence of pH and ionic strength on dye's removal is illustrated in figure 9 for ALG-DY54 system. It is observed that removal is increased when pH moves down and ionic strength is high. The lower pH value considered in this study was determined by DY54 solubility, pH values lower than 10.8 promote precipitation of the dye.

The interaction between alginate and DY54 is favored under "acidic conditions", due to anionic nature of the species involved. At lower pH values the negative net charge of both molecules DY54 and alginate anion is diminished thus favoring their interaction. The ionic strength of the solution favors hydrophobic interaction between DY54 and alginate molecules conducting to a higher removal of the dye at high ionic strength values.

In the case of XANT-DY54 system, two factors determine the DY54 removal by xanthan: solubility of DY54 molecules and repulsion between xanthan and DY54 molecules (Figure 10). First is favored to high pH values and binding of DY54 molecules to xanthan molecule is promoved. When pH is ele-

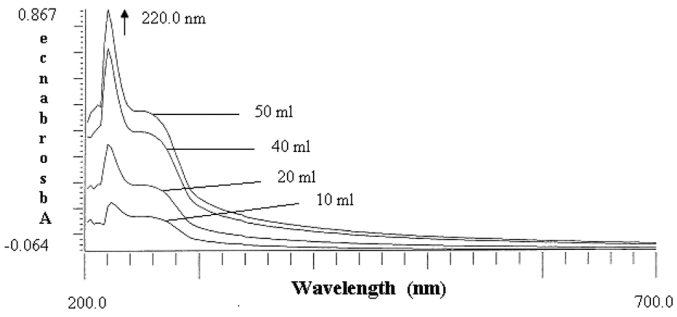

Fig. 8. UV-Visible absorption spectra of diluents solution when xanthan solution (1%w/v) was added.

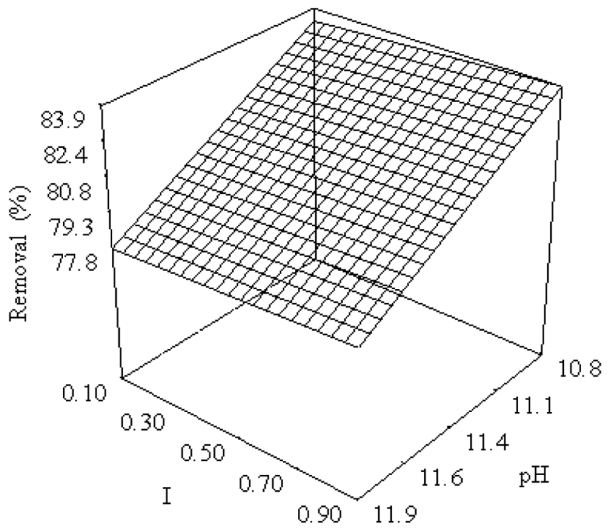

Fig. 9. Schematic diagram of removal of DY54 as function of pH and ionic strength by alginic acid.

vated repulsion increases and the number of molecules bounded to xanthan is diminished. Figure 10 shows that the equilibrium between these two factors is ubicated in pH = 11.40.

The structure of Xanthan molecule is different from that of alginate [20]. It has branches that envelop principal chain formed by glucose and the negative charge of its molecule is provided by piruvate and glucuronate moieties. Xanthan monomer has a negative charge lower than that observed in alginic acid at experimental conditions performed in this work. This means that repulsion between DY54 and xanthan molecules is reduced in comparison with ALG-DY54 system and for consequence removal of DY54 by xanthan is more effective. In the same way that occurred in ALG-DY54 system, removal of DY54 is favored at high ionic strength

Sorption Isotherms

The optimal conditions obtained from the previous section in this same work (sorption studies) were used to obtain the sorption isotherms of both systems ALG-DY54 and XANT-DY54 (Figure 11). qe is defined as mass (mg) of dye bounded to a defined amount of biopolymer (g) and Ce is the equilibrium concentration of DY54 unbounded to biopolymer (mg/L). At first instance seems to be that isotherms follow a Nernst model which is applied in dyeing of textile fibers [26]. The adsorption isotherm is described in terms of a dissolution mechanism and the dye concentration in fiber is proportional to its concentration in the aqueous medium. However it is considered that this model is very simple to describe the phenomenon that occurred in the systems studied in this work.

We use the following models in an attempt to describe the experimental data: Langmuir (27), Freundlich (28) and Zimm-Bragg (29). The Langmuir isotherm is represented by following equation:

$$q_e = K_L C_e / 1 + a_L C_e \quad (1)$$

Where:

q_e = Mass of dye retained by unity mass of biopolymer (mg/g)
C_e = Equilibrium free dye concentration (mg/L)
K_L and a_L= Langmuir Constants with following units (L/g) and (L/mg) respectively.

Rewriting the Langmuir equation, we may obtain:

$$C_e/q_e = a_L C_e / K_L + 1/ K_L \quad (2)$$

If C_e/q_e is plotted versus C_e, a straight line is obtained with slope $m = a_L/K_L$ and intercept in y axis equal to $1/K_L$. When this model is applied to both systems, ALG-DY5A and XANT-DY54 (Figures 12a and 12b, respectively), we observed that their behavior do not fit to the Langmuir model.

Freundich developed the following empirical equation:

$$q_e = K_F C_e^{1/n} \quad (3)$$

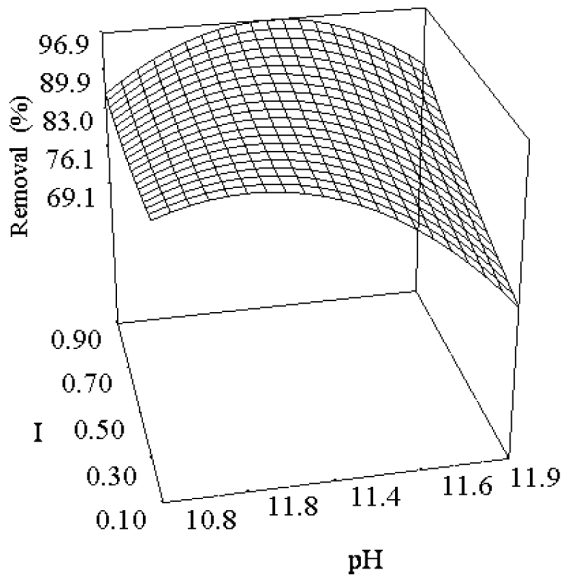

Fig. 10. Schematic diagrams of removal of DY54 as function of pH and ionic strength by xanthan.

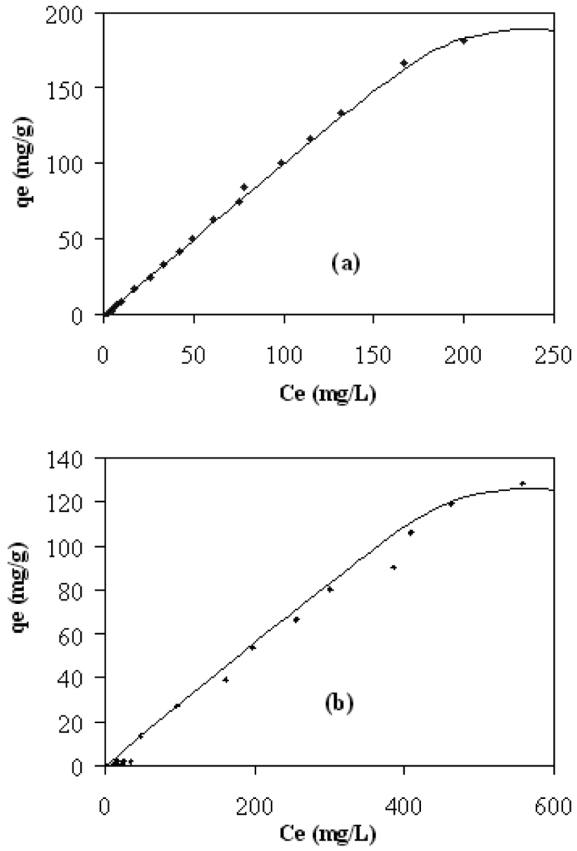

Fig. 11. Sorption isotherms for ALG-DY54 (a) and XANT-DY54 (b) systems.

Where:

q_e = Mass of dye adsorbed by biopolymer (mg/g)
C_e = Dye concentration in aqueous solution (mg/L)
K_F = Freundlich constant (L/g)
1/n = Heterogeneity factor of Freundlich.

Applying logarithm and reordering the equation is obtained the following equation:

$$\ln q_e = 1/n \ln Ce + \ln K_F \quad (4)$$

When ln q_e is plotted versus ln C_e, a straight line is obtained with slope m = 1/n and intercept in y axis equal to ln K_F. In order to elucidate the behavior of our systems (ALG-DY54 and XANT-DY54), we tabulated our experimental data within this model (Figures 13a and 13b, respectively).

Apparently this model describes in better manner the experimental results than do the Langmuir model. But evidently both plots show that a straight line do not fit adequately to experimental data. To define which model fit in the best way, we performed an optimization of parameters using Statistica® software as described in experimental section and the results obtained are reported in Table 1.

The respective plots of Langmuir and Freundlich obtained with the parameters reported in this table were plotted (Figures 14 and 15). If we evaluate the influence of varying the parameters K_L and a_L within the Langmuir model, these may lead to different plots. When both parameters are positive it is obtained the graph showed in Figure 16.

In contrast, when a_L take values <0 the resultant curve is partially located under the zero of y axis (the values of qe obtained are lower than zero). Is important to note that as a_L values decreases the fraction of curve that rises to values of qe greater than zero increases (Figure 17). In this way when a_L=-0.01 the Langmuir plot begins to change drastically its location and concavity (Figure 18). For our particular case, in which the values of K_L = 0.3755 and a_L = -0.003449 (these values were obtained with the optimization process) the plot is included in the same figure, and from which we can infer that our data does not fit this model. Although the value of K_L is allowed, the negative value of a_L means a saturation value of qe smaller than zero, which physically is impossible.

Figure 19 represents the Freundlich plot with n = 1 and K_F values > 0. From this figure is evident that when n = 1 Freundlich equation reduces to q = K_F Ce.

In the particular case where n < 1 with K_F > 1 the Freundlich plot changes drastically (Figure 20), and the resulting plot appears like an "exponential graph". The values derived from global optimization are the following: K_F = 0.2346 and n = 0.7564 and the resulting plot is represented in Figure 15 as was mentioned above. It is clear that Freundlich model fit more adequately to experimental results but the difference between theoretical and experimental curves is evident. From here, we must find another model that describes experimental data in a better way than Langmuir and Freundlich models do.

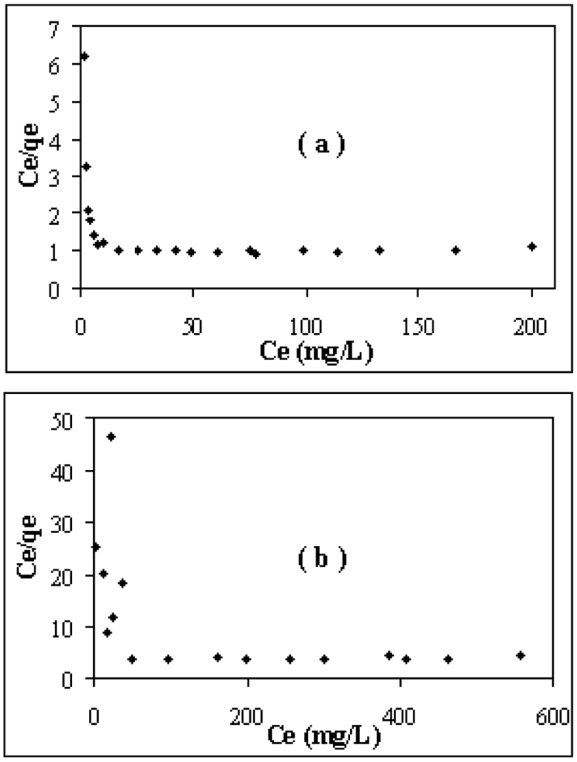

Fig. 12. Plot of C_e/q_e versus C_e to ALG-DY54 system (a) and XANT-DY54 system (b).

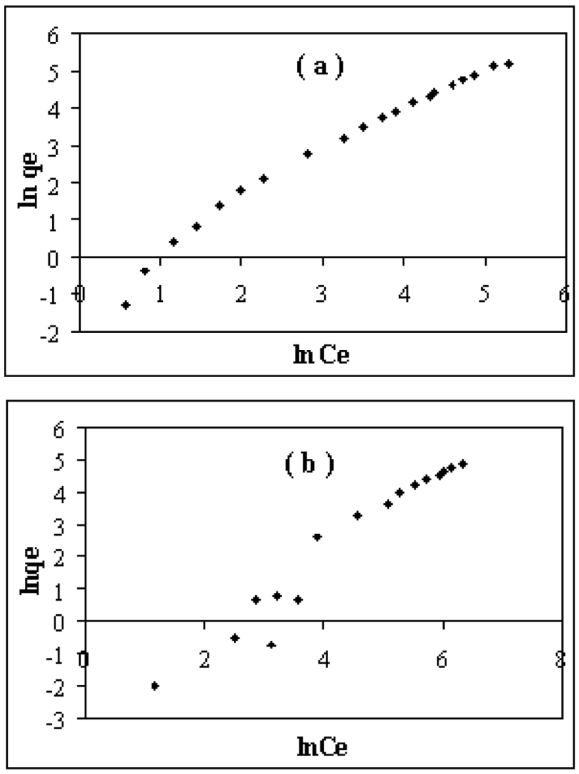

Fig. 13. Plot of lnqe versus ln Ce to obtain Freundlich parameters (K_F and 1/n parameters) in systems (a) ALG-DY54 and (b) XANT-DY54.

Table 1. Parameters evaluated when different models were applied to ALG-DY54 and XANT-DY54 systems.

System / Model	ALG-DY54			XANT-DY54		
	Value of Parameters	Average error	R^2	Value of Parameters	Average error	R^2
Langmuir	K_L = 0.3755 a_L = -0.003449	48.13 %	0.7445	K_L = 0.04266 a_L = -0.001519	55.8 %	0.4344
Freundlich	K_F = 0.2346 n = 0.7564	26.11 %	0.8694	K_F = 0.00550 n = 0.61057	40.16 %	0.8815
Zimm-Bragg	Ku = 3000 U = 4	16.6 %	0.9878	Ku = 900 U = 2	65.84 %	0.9811

Originally Zimm-Bragg Theory was proposed to model conformational changes in proteins [29]. Later on Schwarz-Balthasar [30] and Satake-Yang [31] adapted it to describe binding of molecules as proflavine and acridine orange to polypeptides. The plot of ß (binding coefficient, defined as fraction of polymer sites occupied by dye divided by total potential sites of binding) versus log Ce results on a sigmoidal curve. In Figures 21a and 21b the plots of ALG-DY54 and XANT-DY54 systems are represented.

It was proposed [30,31] that two processes are responsible for aggregates formation: Nucleation and aggregation. Nucleation is the process in which one dye molecule binds to a site adjacent to a site already occupied by other dye molecule; this step is determined by the magnitude of K_u. This process is represented by the following equation:

$$K_u = (DD)/(ED)(D) \quad (5)$$

Where D denotes two adjacent sites occupied by two DY54 molecules and E indicates an empty site onto polymer. The cooperativity parameter u, is defined as:

$$u = (DD)\,(EE)/\,(DE)^2 \quad (6)$$

This equilibrium parameter is about the aggregation process of dye molecules bounded to the polymer.

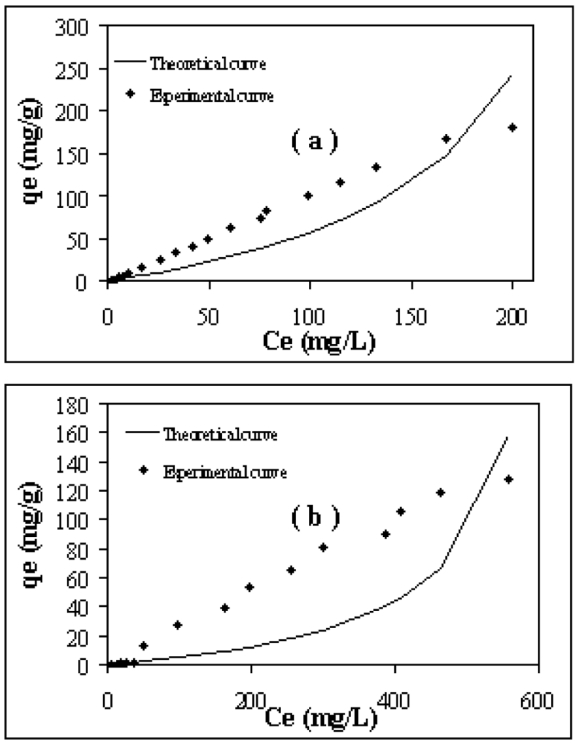

Fig. 14. Comparison of experimental data with Langmuir Isotherm for ALG-DY54 system (a) and XANT-DY54 system (b).

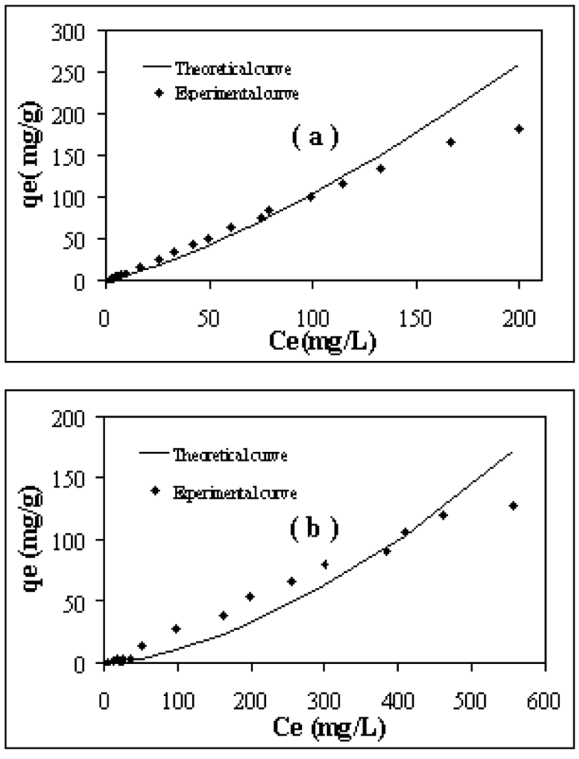

Fig. 15. Comparison of experimental data with Freundlich Isotherm for ALG-DY54 system (a) and XANT-DY54 system (b).

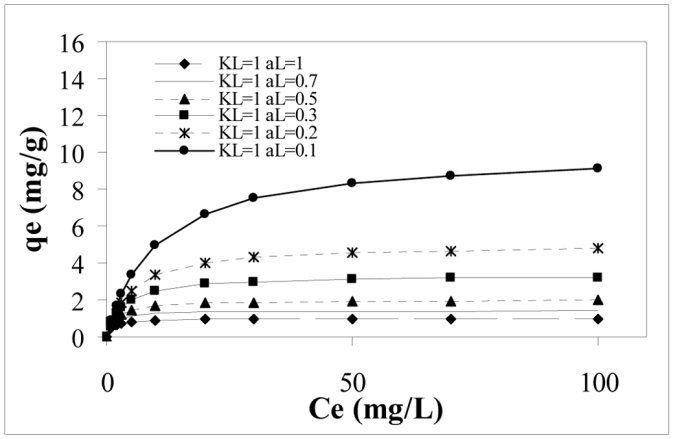

Fig. 16. Langmuir Plot obtained with K_L and a_L parameters are both positive.

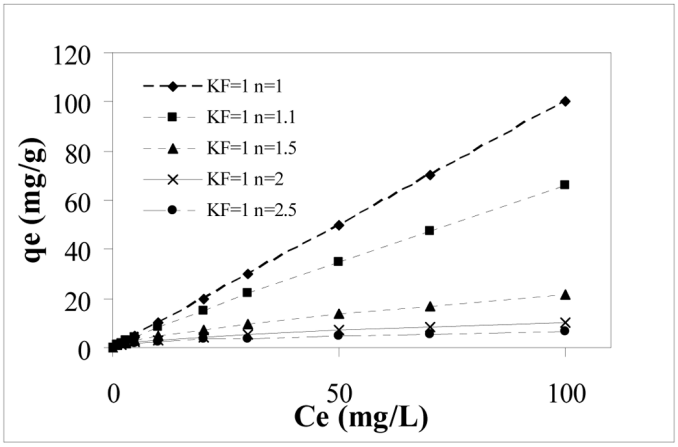

Fig. 19. Freundlich Plot obtained with K_F positive and $n = 1$.

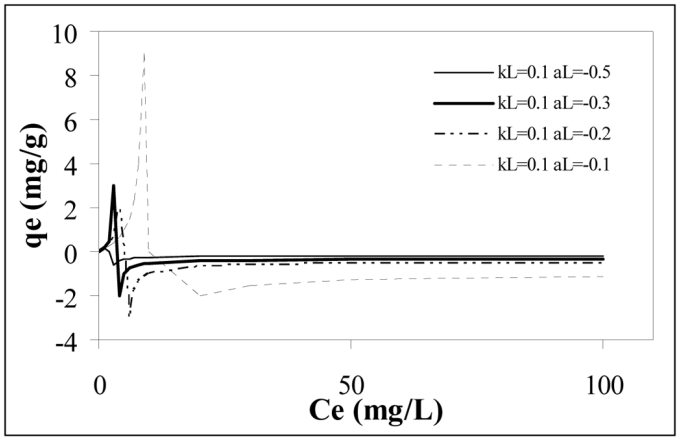

Fig. 17. Langmuir Plot obtained with K_L positive and values of a_L = -0.1.

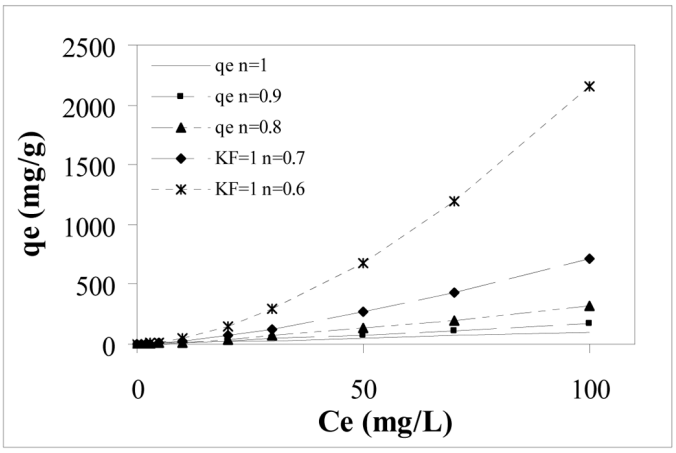

Fig. 20. Freundlich Plot obtained with K_F positive and $n = 1$.

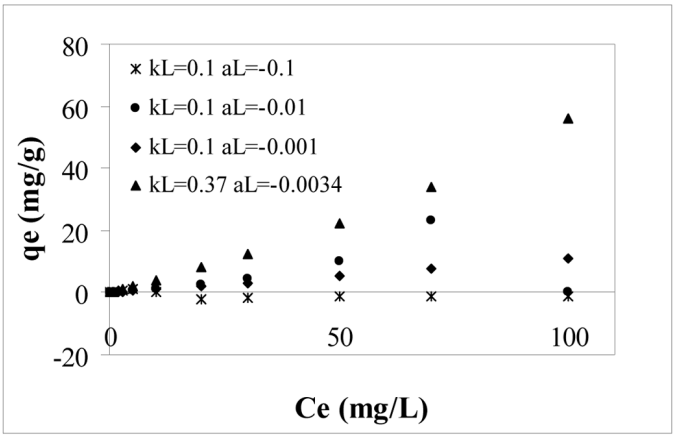

Fig. 18. Langmuir plot obtained with K_L positive and values of a_L = -0.001.

The equation that relates β with K_u and u is the following:

$$\beta = 1/2[1+\{s-1 / [(1-s)^2 + (4s/u)]^{1/2}\}] \quad (7)$$

With $s = K_u C_{DY54}$, and C_{DY54} as the concentration of unbounded DY54 that remains in solution in the equilibrium state. The parameter K_u and u are obtained from the following equations:

$$C_{e\,in}\,\beta = 0.5 = 1/K_u \quad (8)$$

$$D\beta/d \log C_{e\,in}\,\beta = 0.5 = u^{1/2}/4 \quad (9)$$

Using K_u and u as adjustable parameters one can find the best concordance between experimental data and Equations 7-9. The following values of K_u and u were obtained: system ALG-DY54: K_u = 3000 Kg/mol and u = 4; system XANT-DY54 system K_u = 900 Kg/mol and u = 2. These values were substituted in equation 7 in order to obtain the binding

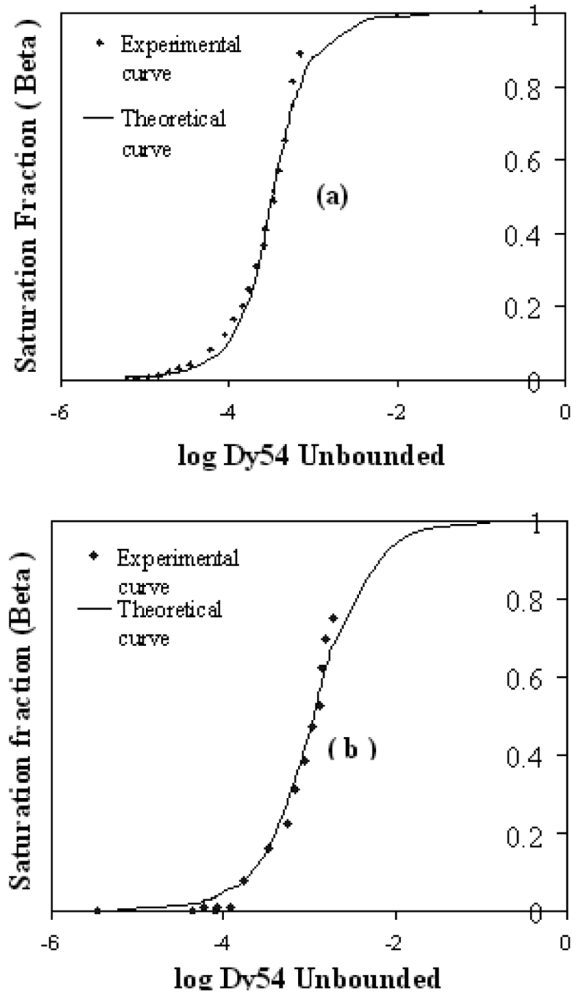

Fig. 21. Zimm-Bragg isotherms for ALG-DY54 system (a) and XANT-DY54 system (b).

isotherms. In Figure 21a and 21b theoretical curves are represented using these values of K_u and u for ALG-DY54 and XANT-DY54 systems respectively. Although the average error is big for both systems, the determination coefficient values suggest that Zimm-Bragg model is the most adequate to ALG-DY54 and XANT-DY54 systems (see Table 1). We do believe that the high values in the average error found in XANT-DY54 system is due to high turbidity of biopolymer solution caused by the presence of little particles of this compound that remain in solution even after centrifugation was done, but in contrast the value of R^2 reinforces the hypothesis that Zimm-Bragg model fits best our experimental data.

Recently different research groups [32-37] have found that this model describes adequately the adsorption isotherm of surfactant-polyelectrolyte systems. Goddard [38] has published that addition of polyelectrolyte to surfactant in an aqueous system decrease the critical micelle concentration (cmc) defined as the minimal concentration of surfactant to form micelles in aqueous solution, and this phenomenon was due to nucleation and aggregation processes which were favored by the presence of polymers. In all cases the surfactant- polyelectrolyte systems were described by Zimm-Bragg model.

The values of K_u and u suggest that in the ALG-DY54 system both processes, nucleation and aggregation are stronger than those encountered in XANT-DY54 system (see K_u and the u values for these systems). It is believed that due to the differences in the degree of stiffness (Length persistence Lp = 120 nm for xanthan [39] and Lp = 5-17 nm for alginic acid [40,41]) among xanthan and alginic acid, being alginic acid more flexible, the nucleation and aggregation processes are favored on this polymer thus its removal capacity is enhanced.

There is no data reported in literature regarding alginate-dye and xanthan-dye systems for K_u and u parameters therefore no possible comparison can be made. Blackburn [42] reported values of punctual studies of color removal promoted by reactive red 238, direct black 22 and acid blue 193 by alginate. However this study does not include adsorption isotherms and in consequence the cooperativity phenomenon of those systems was not defined.

Nasr et al. [43] conducted studies to define the adsorption isotherms for modified alginate. The adsorption capacity of modified alginate was evaluated depending upon the removal of C. I. Basic Red 18 and C. I. Basic yellow 11 dyes. They applied Langmuir and Freündlich isotherms and observed a good agreement between both models and experimental data. We do believe that due to the heterogeneous nature of Nasr´ system, the nucleation and aggregation processes involved in Zimm-Bragg model were not observed.

In an attempt to describe the mechanism for the aggregation phenomenon, we focused on the effect of the ionic strength of the solution. An increase of the ionic strength will increase the hydrophobic interactions of DY54 molecules, thus facilitating the aggregation process. Hayakawa and Kwak [34] reported that increasing the ionic strength will favor aggregation of cationic surfactants when they are in contact with sodium dextran sulfate or sodium poly (styrenesulfonate). In agreement with Hayakawa´s work, our results show that high ionic strength promotes greater adsorption of DY54 by both biopolymers. DY54 molecule has a considerable hydrophobic character due to aromatic rings, therefore an increase of the ionic strength of the solution induces formation of "clusters" on biopolymer surface. Studies realized in our laboratory (still not published) indicate that while in the solid state DY54 exists only as the enol tautomer (Figure 22), in solution, both forms are present. In organic solvents enolic tautomer is favored and in aqueous solution keto form predominates.

In this sense the main infrared absorption bands of sodium alginate, DY54 and ALG-DY54 are observed in Figure 23 and summarized in Table 2. We can observe two main absorption bands located at 1656 cm^{-1} and 1547 cm^{-1}, which correspond to C=O and C=C vibrations respectively of enol tautomeric form. Figure 23c represents the FT-IR spectrum of ALG-DY54. The absorption band observed at 3421 cm^{-1} indicates the presence of hydrogen bonds in ALG-DY54. It is important to remark that this spectrum also shows a protonated carboxylate group (1736 cm^{-1}). This group was protonated

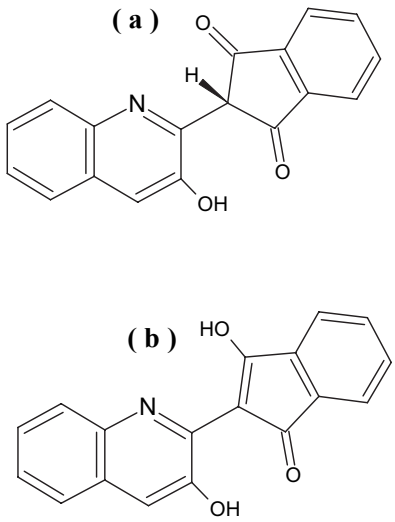

Fig. 22. Tautomeric forms of DY54: Keto (a) and enol (b).

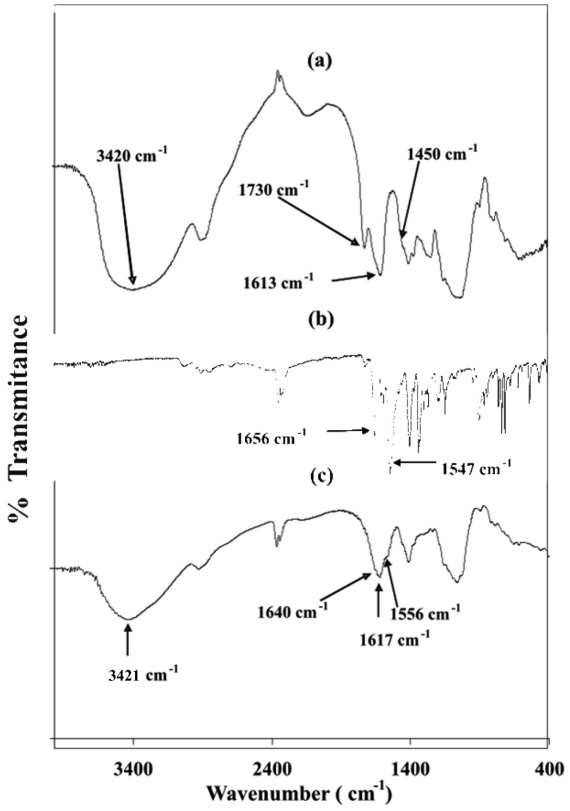

Fig. 23. FTIR spectrum of (a) alginic acid as sodium salt, (b) DY54 and (c) ALG-DY54.

as a result of the precipitation of ALG-DY54 with hydrochloric acid.

Comparison of the FT-IR spectra of DY54 and ALG-DY54 we observed that the principal differences among them are the shift of the C=O absorption band (1656 cm^{-1} for DY54 and 1620 cm^{-1} for ALG-DY54) and the disappearance of the peak encountered at 1547 cm^{-1} in DY54 spectrum (Table 2).

Table 2. FT-IR Data of ALG-DY54 Product.

FTIR signal	Alginate	DY54	ALG-DY54	Observations
ν (O-H)	3450 cm^{-1}		3421 cm^{-1}	Hydrogen bonding still exists in ALG-DY54
ν_{as}(COO)	1614 cm^{-1}		1736 cm^{-1}	Carboxylate group protonated
ν_{s}(COO)	1420 cm^{-1}		1420 cm^{-1}	Without changes
ν(C=O)		1656 cm^{-1}	1620 cm^{-1}	Hydrogen bonding where C=O of DY54 is involved
			1646 cm^{-1}	A few of DY54 is encountered in enol form.
ν(C=C)		1547 cm^{-1}	Disappears	Keto form of DY54 is present

This suggests that keto form is the principal chemical specie that exists in ALG-DY54 system, however one peak located at 1646 cm^{-1} indicates that a considerable amount of DY54 remains in the powder of ALG-DY54 as enol form. In both cases the DY54 molecules presumably can be interacting with biopolymer through hydrogen bonding.

In the same order Figure 24 shows the IR spectra of xanthan, DY54 and XANT-DY54 compounds and their respective signals are summarized in Table 3. Is remarkable that due to a basic pH solution, the acetyl group was liberated by saponification and its signal does not appear in spectrum. Although the signal corresponding to asymmetric vibration of carboxilate groups from pyruvate and glucuronate moieties are located at 1617 cm^{-1}, it is thought that the (C=O) vibration of DY54 has moved from 1656 cm^{-1} to this same wavenumber value (1617 cm^{-1}) upon complex XANT-DY54 formation. Unfortunately, it is difficult the identification of its signal in the IR spectrum of XANT-DY54 due to its "low concentration" in this compound. The presence of the peaks encountered at 1640 cm^{-1} and 1556 cm^{-1} suggest that enol tautomer of DY54 is present in the XANT-DY54 compound.

Raman spectra of DY54, ALG-DY54 and XANT-DY54 are depicted in Figure 25. For DY54 one main peak is observed at 1376 cm^{-1}, which corresponds to C-C=C vibration (Figure 25 a). It is observed a shift of this peak to 1080 cm^{-1} after DY54 is bonded to alginate (Figure 25 b). We propose that a change in structure of DY54 has occurred (Figure 26). The enol form of DY54 predominates in the solid state and both tautomers may be present in aqueous solution. When DY54 interacts with alginic acid and xanthan, the vibration of

Table 3. FT-IR Data of XANT-DY54 Product.

FTIR signal	Xanthan	DY54	XANT-DY54	Observations
ν(O-H)	3420 cm^{-1}		3381 cm^{-1}	Hydrogen bonding still exists in XANT-DY54
ν(C=O) acetyl group	1730 cm^{-1}		Almost Disappears	Free acetyl groups by saponification reaction of xanthan.
ν_{as}(COO) pyruvate and glucuronate groups	1613 cm^{-1}		1617 cm^{-1}	Carboxylate group as sodium salt (no changes)
ν_{s}(COO) pyruvate and glucuronate groups	1450 cm^{-1}		1450 cm^{-1}	Without changes
ν(C=O)		1656 cm^{-1}	1640 cm^{-1}	Something of enol form of DY54 is present in product.
			1617 cm^{-1}	Hydrogen bonding where C=O of DY54 is involved
ν(C=C)		1547 cm^{-1}	1556 cm^{-1}	Something of enol form of DY54 is present in product.

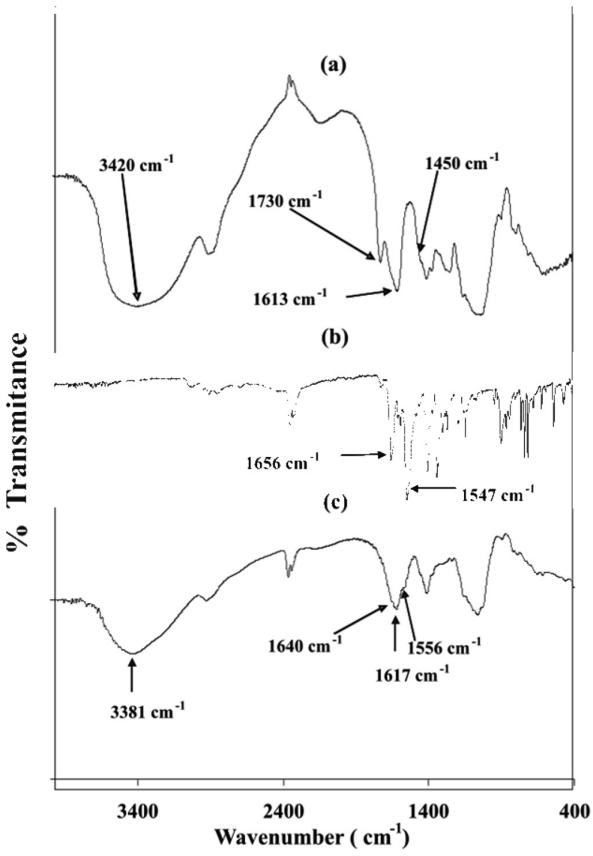

Fig. 24. FTIR spectrum of (a) xanthan as sodium salt, (b) DY54 and (c) XANT-DY54.

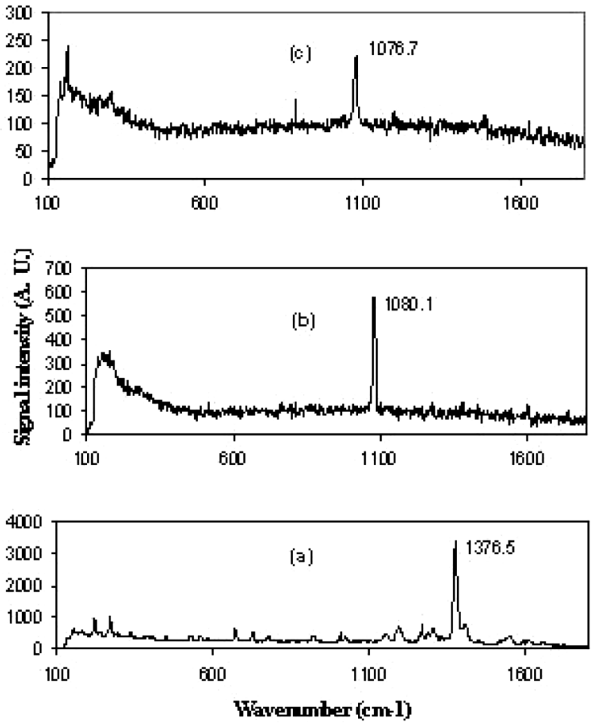

Fig. 25. Raman spectra of (a) DY54, (b) ALG-DY54 and (c) XANT-DY54.

C-C=C disappears and the vibration C-C-C appears in Raman spectra of ALG-DY54 and XANT-DY54 (Figures 25b and 25c, respectively), suggesting that keto form is the principal tautomer involved in DY54 removal when biopolymers xanthan and alginic acid are used.

In general our results indicate that the interaction of DY54 with both biopolymers alginic acid and xanthan is similar. When ALG-DY54 and XANT-DY54 are washed with ethanol solution (70% v/v), DY54 desorbs from the complexes due to the strongest interaction among ethanol and polymer (displacement of DY54 by ethanol). This finding, supported by the Infrared and Raman studies, suggests that the interaction responsible for removal of DY54 by alginic acid and xanthan is through hydrogen bonding. Thus, we propose that the hydrox-

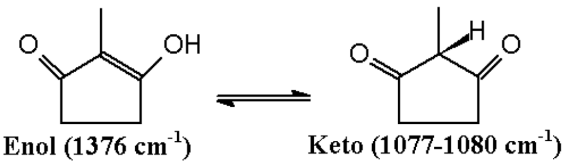

Fig. 26. Fraction of structure of DY54 involved in equilibrium of enol and keto tautomers and their respective values of (C-C-C) vibration in Raman spectrum.

yl groups of both biopolymers (alginic acid and xanthan) are involved in DY54 removal. In addition, hydrophobic interactions are responsible for the formation of DY54 aggregates in accordance with Ren and Li reports [44,45]. The results from Fluorescence and Dynamic Light Scattering Studies realized by the Ren's group, showed formation of aggregates when cationic surfactants were mixed with alginate in aqueous solutions. Li's group observed the aggregation process in solutions where cationic surfactant Nonyphenyloxypropyl β-Hydroxyltri methylammonium as bromide salt was in contact with xanthan in aqueous medium. They also conducted computational studies using MesoDyn method to confirm experimental findings. Both groups concluded aggregation phenomenon contributes to increase the removal capacity of biopolymers.

In view of anterior it is clear that an understanding of the interaction dye-biopolymer is fundamental in order to increase the efficiency of pollutants removal from water. These studies set the basis to explore chemical or biotechnological ways to modify the chemical structure of biopolymers alginic acid and xanthan in order to improve their ability of dyes removal.

Experimental

Chemicals. The dye DY54 was purchased as commercial mixture (Mardupol Co.). Biopolymers alginic acid and xanthan both as sodium salt were obtained from Sigma and were used without further purification. All solvents used were HPLC grade and were from J.T. Baker except distilled water. Potassium bromide (spectrophotometric grade) and silica gel 60 (230-400 mesh) were supplied by Merck.

Dye purification. DY54 was purified in a chromatography column with silica gel 60 using chloroform as eluent. Purity grade was tested by HPLC.

UV-Visible studies. Spectra of DY54 solution (from 200 to 700 nm) were obtained at pH values higher than 10.8 because solubility of dye under this pH value decreases drastically.

Solutions of alginate and xanthan gum (aliquots of 1 % biopolymer solution: 3, 5, 10, 20, 40 and 50 mL; pH = 11.67) were added to 4.8 x 10^{-5} M DY54 aqueous solution (100 mL; pH = 11.67) and spectra were acquired. In the same way aliquots of both biopolymer solutions were added to basic solution without dye to know the polymer effect on the UV-Visible spectrum.

Optimization of sorption conditions. The dye DY54 was dissolved in a basic solution (pH = 12.15) of sodium hydroxide and adjusted to 125 ppm. An aliquot of this solution (40 mL) was added to a 50 mL solution of biopolymer (1%). Three samples were prepared with pH adjusted (using HCl and/or NaOH) to 10.8, 11.4 and 12.0 respectively. For each pH value, solutions with different ionic strength were prepared by addition of sodium chloride crystals. The ionic strength values were, I = 0.1M, 0.5M and 0.9M. The final volume of all samples was 100 mL and final concentration of DY54 was 50 ppm (all samples were carried out in triplicate). Samples were cap sealed and shaken (200 rpm) for 40 h at 27 °C in darkness. The free dye quantification was done in two different ways:

1) ALG-DY54 SYSTEM. Hydrochloric acid (20% v/v) was added to each sample until a pH = 1.0 was reached. A precipitate of ALG-DY54 and unbounded dye remained in solution. Distilled water was added to complete final volume of 100 mL. All samples were incubated for 20 h at room temperature (27 ºC), supernatant was centrifuged to 9000 g for 20 min and free dye concentration was determined by interpolation of absorbance measured at 373 nm in a calibration curve.
2) XANT-DY54 system. Distilled water was added to complete final volume of 100 mL and solution was shaken slightly. Samples remained 20 h (27 °C) and supernatant was centrifuged to 9000 g, for 20 min. free dye concentration was determined in the same way that ALG-DY54 system.

Sorption isotherms. A 2000 ppm DY54 solution was prepared at pH 12.15 and ionic strength of 0.9M. Solutions of different concentration were prepared from it: 5-2000 ppm.

After addition of 0.5 g of biopolymer powder to each solution all recipients were cap sealed and maintained for 3h at room temperature to allow hydration. Afterward samples were shaken (200 rpm) for 40 h at 27 °C in darkness. Finally free dye concentration was determined as mentioned above.

Determination of the theoretical values of Langmuir, Freundlich and Zimm-Bragg parameters.

The parameters of each model were obtained through the Statistica® software. The function corresponding to each model was introduced to software and the proposed values corresponding to models of Langmuir, Freundlich and Zimm-Bragg were assigned to start the optimization process in this software. This process was done using the following function as optimization parameter:

$$L = [(\text{observed value} - \text{theoretical value})/(\text{observed value})]^2$$

The software ends the optimization process when L value is at minimum and the optimized values (determination coef-

ficient (R^2), Average error and the respective values of parameters of each model) are displayed as a result report.

Infrared and Raman studies. A sample of pure DY54 powder was used to obtain the Raman spectrum of this dye.

The analyzed powders (ALG-DY54 and XANT-DY54) were isolated and purified as follows: ALG-DY54 obtained from the isotherm was washed out five times with distilled water to eliminate free DY54 in supernatant, filtered off, dried at 50°C for 24 h and finally grounded. XANT-DY54 gel was washed out in the same way as previous product but it was not filtered off.

For infrared spectra all samples DY54, ALG-DY54 and XANT-DY54 were prepared as potassium bromide pellets and their FT-IR spectra were obtained in 4000-400 cm^{-1} range.

Raman spectra did not require any sample processing. The powder of DY54, ALG-DY54 and XANT-DY54 were used to obtain Raman spectra in 100-1800 cm^{-1} range. Raman spectra (830 nm) of biopolymers were performed but due to fluorescence of both biopolymer ALG and XANT molecules was not possible their acquisition.

Analitycal procedures. HPLC was performed in a Perkin-Elmer chromatograph (Perkin-Elmer, series 200) equipped with a 150 x 10 mm C_{18} reverse phase 5mm column (Supelco) and a UV-Visible detector series 200 using a wavelength of 370 nm . The sample was eluted with acetonitrile at 1 mL/min.

UV-Visible studies were carried out in a Thermospectronic spectrophotometer (model Genesys 2). Spectra were obtained in from 200 to 700 nm.

Ionic strength of dye solutions was adjusted measuring electric conductivity of solution with a Corning Conductimeter.

FT-IR measurements were made in a FT-IR Perkin-Elmer spectrometer (Perkin-Elmer 1600 series).

FT-IR spectra were obtained in 4000-400 cm^{-1} range. Raman spectra were obtained in a MicroRaman system (Renishaw 1000B) with an excitation wavelength of 830 nm. Raman spectra were obtained in 100-1800 cm^{-1} range.

Acknowledgements

We acknowledge the support of Consejo Nacional de Ciencia y Tecnología, México (Grants No. 063581 and 054792). Thanks to Ph.D. Iliana Medina-Ramírez for document improvement.

References

1. Willmott, N.; Guthrie, J.; Nelson, G. *J. Soc. Dye Colour.* **1998,** *114*, 38-41.
2. Baughman, G. L.; Weber, E. J. *Environ. Sci. Technol.* **1994,** *28*, 267-276.
3. Goncalves, I. M. C.; Gomes, A.; Brás, R.; Ferra, M. I. A.; Amorim, M. T. P.; Porter, R. S. *J. Soc. Dye Colour.* **2000,** *116*, 393-397.
4. Özcan, A. S.; Clifford, A. A.; Bartle, K. D. *J. Chem. Eng. Data* **1997,** *42*, 590-592.
5. Joung, S. N.; Yoo, K.-P. *J. Chem. Eng. Data* **1998,** *43*, 9-12.
6. Guzel, B.; Akgerman, A. *J. Chem. Eng. Data* **1999,** *44*, 83-85.
7. Lee, J. W.; Min, J. M.; Bae, H. K. *J. Chem. Eng. Data* **1999,** *44*, 684-687.
8. Sung, H.-D.; Shim, J.-J. *J. Chem. Eng. Data* **1999,** *44*, 985-989.
9. Shinoda, T.; Tamura, K. *J. Chem. Eng. Data* **2003,** *48*, 869-873.
10. Hou, A.; Dai, J. *Color. Technol.* **2005,** *121*, 18-20.
11. Holme, I., in: *Handbook of Technical Textiles*; Horrocks, A. R.; Anand, S. C., Eds. Woddhead Publishing, Cambridge **2000**, 187-222.
12. Alí, M. F., in: *Handbook of Industrial Chemistry, Organic Chemicals*. Alí, M. F.; El-Alí, B. M.; Speight, J. G., Eds; McGraw-Hill, New Work. **2005**, 259-288.
13. Özacar, M.; Sengil, I. A. *Environ. Geol.* **2004,** *45*, 762-768.
14. Lin, S. H. *J. Chem. Tech. Biotechnol***. 1993,** *57*, 387-391.
15. Ramakrishna, K. R.; Viraghavan, T. *Waste Manag***. 1997,** *17*, 483-488.
16. Ramakrishna, K. R.; Viraghavan, T. *Water Sci Tech.* **1997,** *36*, 189-196.
17. Draget, K. I., in: *Handbook Hydrocolloids*; Phillips, G. O.; Williams, P. A., Eds.; Woddhead Publishing, Cambridge, **2000**, 379-395.
18. Grant, G. F.; Morris, E. R.; Rees, D. A.; Smith, P. J. C.; Thom, D. *FEBS Lett***. 1973,** *32*, 195-198.
19. Glazer, N. A.; Nikaido, H. W. H. *Microbal Biotechnology, Fundamentals of Applied Microbiology*; W. H. Freeman and company, New York, **1995**, 272-277.
20. Jansson, P. E.; Kenne, L.; Lindberg, B. *Carbohydr. Res.* **1975,** *45*, 275-282.
21. Papariello, G. J.; Commanday, S. *Anal. Chem.* **1964,** *36*, 1028-1030.
22. Brode, W. R. *J. Am. Chem. Soc***. 1924,** *46*, 581-596.
23. Garzón, G. A. *Acta Biol. Colomb***. 2008,** *13*, 27-36.
24. Levillain, P.; Fompeidye, D. *Anal. Chem.* **1985,** *57*, 2561-2563.
25. Pal. M. K.; Mandal, N. *Biopolymers* **1990,** *29*, 1541-1548.
26. Burkinshaw, S. M. *Chemical Principles of Synthetic Fibre Dyeing*: Blackie Academic and Professional, London, **1995**, 180-185.
27. Langmuir, I. *J. Am. Chem. Soc***. 1916,** *38*, 2221-2295.
28. Freundlich, H. M. F. *Z. Phys. Chem.* **1906,** *57*, 385–470.
29. Zimm, B. H.; Bragg, J. K. *J. Chem. Phys***. 1959,** *31*, 526-535.
30. Schwarz, G.; Balthasar, W. *Eur. J. Biochem***. 1970,** *12*, 461-467.
31. Satake, I.; Yang, J. T. *Biopolymers* **1976,** *15*, 2263-2275.
32. Hayakawa, K.; Kwak, J. C. T. *J. Phys. Chem.* **1982,** *86*, 3866-3870.
33. Hayakawa, K.; Santerre, J. P.; Kwak, J. C. T. *Macromolecules* **1983,** *16*, 1642-1645.
34. Hayakawa, K.; Kwak, J. C. T. *J. Phys. Chem.* **1983,** *87*, 506-509.
35. Malovikova, A.; Hayakawa, K.; Kwak, J. C. T. *J. Phys. Chem.* **1984,** *88*, 1930-1933.
36. Okuzaki, H.; Osada, Y. *Macromolecules* **1994,** *27*, 502-506.
37. Jain, N.; Trabelsi, S.; Guillot, S.; McLoughlin, D.; Langevin, D.; Letellier, P.; Turmine, M. *Langmuir* **2004,** *20*, 8496-8503.
38. Goddard, E. D., in: *Principles of Polymer Science and Technology in Cosmetic and Personal Care*. Desmond, E. Ed. Marcel Dekker Inc. New York, **1999**, 152-164.
39. Sato, T.; Norisuye, T.; Fujita, H. *Polym. J***. 1984,** *16*, 341-350.
40. Strand, K. A.; Bøc, A.; Dalberg, P. S.; Sikkeland, T.; Smidsrød, O. *Macromolecules* **1982,** *15*, 570-579.
41. Smidsrød, O.; Haug, A. *Acta Chem. Scand***. 1968,** *22*, 797-810.
42. Blackburn, R. S. *Environ. Sci. Technol.* **2004,** *38*, 4905-4909.
43. Nasr, M. F.; Abo El-Ola, S. M.; Ramadan, A.; Hashem, A. I. *Polym.-Plast. Technol. Eng.* **2006,** *45*, 335-340.
44. Ren, B.; Gao, Y.; Lu, L; Liu, X.; Tong, Z. *Carbohyd. Polym.* **2006,** *66*, 266-273.
45. Li, Y. M.; Xu, G. Y.; Chen, A. M.; Yuan, S. L. ; Cao, X. R. *J. Phys. Chem. B*. **2005,** *109*, 22290-22295.